

Search for new superconductors in the Y-Ni-B-C system

B. Knigge,^{a)} A. Hoffmann,^{b)} D. Lederman,^{c)} D. C. Vier, S. Schultz, and Ivan K. Schuller
Physics Department 0319, University of California–San Diego, La Jolla, California 92093-0319

(Received 3 September 1996; accepted for publication 19 November 1996)

We have searched for superconductivity in a wide variety of stoichiometries in the Y-Ni-B-C system, using $Y_x(\text{NiB})C_y$ phase spread alloy thin films and the magnetic field modulated microwave absorption technique. The superconducting critical temperature (T_c) varies with the stoichiometry, showing the highest T_c for a Y/Ni ratio of 1/2, attributed to the $\text{YNi}_2\text{B}_2\text{C}$ phase. We found no other superconducting phases with a T_c higher than 10 K. Furthermore, a search in $Y_x\text{NiB}(\text{C}_{1-z}\text{N}_z)_y$ and $Y_x\text{NiBN}_y$ phase spread alloys showed no superconductivity. © 1997 American Institute of Physics. [S0021-8979(97)01705-2]

I. INTRODUCTION

Since the initial discovery of the cuprate high temperature superconductors, the search for new superconductors has intensified. A wide variety of materials with a high superconducting critical temperature (T_c) have been discovered, including high T_c cuprates, organic materials, and intermetallic compounds.¹ Because all of these complex materials consist of several elements, the search for new superconductors is very tedious. In order to address this problem, we previously developed a technique useful for the search of new superconductors in complex systems [detection technique for superconductors using phase spread alloys and magnetic field modulated microwave absorption (DSPM)].² Briefly, this method consists of growing “phase spread alloys,” films with a continuously varying composition, and detecting small traces of superconductivity in these films using magnetic field modulated (MFM) microwave absorption. The feasibility and high sensitivity of this method was demonstrated using high T_c cuprates.²

Among the newly discovered intermetallic superconducting compounds are the borocarbides and nitrides. The highest T_c in this class of materials is 23 K for $\text{YPd}_5\text{B}_3\text{C}_{0.3}$.³ The $\text{YNi}_2\text{B}_2\text{C}$ (1221) phase has a bulk T_c of 15.6 K,^{4,5} while the YNiBC (1111) phase was reported to be non-superconducting in bulk.^{5,6} There are also claims of superconductivity with a T_c of 15.9 K for the bulk $\text{YNi}_4\text{B}_4\text{C}$ (1441) phase.⁷ The layered structure of these compounds, consisting of Ni_2B_2 and YC planes, is similar to the structure of the high T_c oxide superconductors,⁸ where the T_c has been claimed to vary with the number of CuO_2 planes per unit cell⁹. Superconductivity was also reported in the boronitride compound $\text{La}_3\text{Ni}_2\text{B}_2\text{N}_3$.¹⁰

In the work described here, we applied the DSPM technique to the search of superconductivity in borocarbide and boronitride films. We found that all borocarbide samples with a T_c greater than 10 K had a significant fraction composed of the $\text{YNi}_2\text{B}_2\text{C}$ phase, and no new phases with a $T_c > 10$ K were discovered. In addition, no superconductivity

was detected in the boronitride films, that is, films grown in a partial nitrogen gas pressure.

II. EXPERIMENT

Y-Ni-B-C phase spread alloy thin films were prepared by simultaneous cosputtering from three sputtering guns. All three sputtering guns (99.5% purity Y, NiB, and C) pointed towards the substrate with the substrate holder in a fixed position above the guns. The films were deposited on MgO (100) substrates ranging in size from 2.5 mm×10 mm to 5 mm×10 mm. The substrates were cleaned ultrasonically in acetone and methanol before bonding them with indium onto the substrate holder. The argon sputtering gas pressure and the substrate temperature were kept constant ($p_{\text{Ar}}=30$ mTorr, $T_s=900$ °C), while the power outputs of the three sputtering guns were varied for each sample. The dc power output ranged from 4 to 12 W for the yttrium gun and from 20 to 41 W for the carbon gun. An rf power supply, set between 12 and 91 W, was used for the NiB gun. After growth some samples were postannealed in a vacuum of 1×10^{-7} Torr at a temperature of 1000 °C.

In order to grow $Y_x\text{NiB}(\text{C}_{1-z}\text{N}_z)_y$ (boronitrides), nitrogen gas was added to the argon sputtering gas. The N_2 partial pressure was varied from 0.2 to 9 mTorr, while the total gas pressure was maintained at 30 mTorr. As we increased the N_2 partial pressure, the carbon power output was reduced stepwise from 20 to 0 W, thus to insure nitrogen incorporation.

The film thickness was determined by measuring several samples with a contact profilometer. The thickness varied slightly depending upon the deposition conditions, being typically 1100 ± 100 Å. The structure of the films was characterized using x-ray diffraction. The x-ray diffraction data from our films were compared with measurements taken on bulk $\text{YNi}_2\text{B}_2\text{C}$, published data,^{6,8} and with simulated powder diffraction patterns of $\text{YNi}_2\text{B}_2\text{C}$ and YNiBC . For the powder diffraction pattern simulation, we used the tetragonal ThCr_2Si_2 structure with $a = b = 3.53$ Å and $c = 10.57$ Å for the $\text{YNi}_2\text{B}_2\text{C}$ phase⁸ and $a = b = 3.6$ Å and $c = 7.6$ Å for the YNiBC phase,⁶ respectively.

The chemical composition of the Y-Ni-B-C phase spread alloys was analyzed with energy dispersive x-ray microanalysis (EDX) and Auger electron spectroscopy, using

^{a)}On leave from the Technische Universität München-Walther Meissner Institut, 85748 Garching b. München, Germany.

^{b)}Electronic mail: hoffmann@ucsd.edu

^{c)}Present address: Physics Department, University of West Virginia, Morgantown, WV 26506-6315.

TABLE I. Change of T_c^μ with increasing substrate temperature T_s . All other deposition parameters are fixed and each sample has the same Y/Ni ratio of 0.5.

| Sample number | T_s (°C) | T_c^μ (K) |
|---------------|------------|---------------|
| 1 | 800 | 11.0 |
| 2 | 850 | 12.4 |
| 3 | 900 | 12.7 |
| 4 | 950 | 13.2 |

polycrystalline $\text{YNi}_2\text{B}_2\text{C}$ as a standard. The Y/Ni ratio varied typically by 10% over the length of the phase spread alloy film, and the values shown in this article represent an average value, which was determined at the center of the film.

The presence of a superconducting phase in our Y-Ni-B-C phase spread alloys was determined using MFM microwave absorption. For these measurements the sample was placed in a TE102 cavity of an electron-spin-resonance spectrometer operating at a frequency of 9.2 GHz. To separate the signal of the sample from that of the cavity, we applied a 20 Oe external dc magnetic field, modulated at 260 Hz with a peak to peak amplitude of 10 Oe. The temperature dependence of the microwave absorption measured this way shows a peak near T_c . The superconducting onset temperature T_c^μ is defined as the temperature above which the MFM microwave absorption signal is reduced below the background noise level. A major advantage of the MFM microwave absorption method, when compared to magnetization or transport measurements, is its high sensitivity, e.g., traces of $\text{YBa}_2\text{Cu}_3\text{O}_7$ as small as $5 \times 10^{-11} \text{ cm}^3$ can be detected.¹¹

In addition to determining T_c^μ with the MFM microwave absorption, we measured the magnetization and the magnetoresistance as a function of temperature and external field for several superconducting samples. Magnetization data were obtained using a SQUID magnetometer, with the samples aligned parallel to the applied external field in order to avoid demagnetizing effects. Transport measurements were performed in a He-flow cryostat with a four point technique.

III. RESULTS AND DISCUSSION

Before attempting the growth of new compounds in the Y-Ni-B-C system, we optimized the growth conditions of the 1221 phase. The deposition rates of the Y, NiB, and C guns were independently adjusted so as to obtain Y-Ni-B-C phase spread alloys close to the 1221 stoichiometry. After this, we optimized the substrate temperature to achieve the highest possible T_c^μ . T_c^μ increased from approximately 11 to 13 K as the substrate temperature increased from 800 to 950 °C (see Table I), while films grown at room temperature were not superconducting. A similar change in T_c^μ was observed by postannealing the samples that were grown at 900 °C at 1000 °C in vacuum. The change of T_c^μ due to postannealing is shown in Table II. Together with the increase of T_c^μ there is a c -axis expansion of up to 1%, approaching the bulk value for the c axis. This is detected by x-ray diffraction (see Table II). After postannealing the films showed a decrease in the c -axis mosaic spread of the 1221 phase, as shown by an

TABLE II. Effect of post annealing for Y-Ni-B-C phase spread alloys. One sample was sequentially annealed several times for 12 min at 1000 °C in vacuum. T_c^μ increases, whereas the Y/Ni ratio stays constant at 0.5. The intensity (I^{004}/I^{200}) of the $\text{YNi}_2\text{B}_2\text{C}$ (004) x-ray diffraction peak normalized to the (200) peak increases, while at the same time the full width at half maximum (FWHM) of the rocking curve of the (004) peak (Γ_{RC}^{004}) decreases.

| Total annealing time (min) | T_c^μ (K) | I^{004}/I^{200} | Γ_{RC}^{004} (degrees) | $2\Theta^{004}$ (degrees) |
|----------------------------|---------------|-------------------|--------------------------------------|---------------------------|
| 0 | 12.7 | 12.6 | 1.5 | 34.03 |
| 12 | 13.2 | 21.1 | 1.2 | 33.98 |
| 24 | 13.5 | 93.3 | 1.0 | 33.90 |

increase in intensity of the (004) peak and a decrease of the rocking curve width (see Table II). These results are similar to the changes observed by Arisawa *et al.* for postannealed $\text{YNi}_2\text{B}_2\text{C}$ films.¹² This might be due to an improved crystallinity of the 1221 phase after annealing and could therefore also explain the increase in T_c^μ .

From EDX we could only determine the Y and Ni content in the Y-Ni-B-C phase spread alloys, since this method is not sensitive to low mass elements. Unfortunately, it proved unreliable to determine the exact carbon content in these phase spread alloys with Auger electron spectroscopy, since carbon is a common surface impurity and the analysis was carried out *ex situ*. Therefore we investigated the change of T_c^μ with various power levels of the carbon sputtering gun. An increased carbon gun power resulted in a higher T_c^μ , and an increase of the Y/Ni ratio. A possible explanation is that with an increased carbon content more YC layers are formed, thus increasing the incorporation of yttrium in the film. At relatively high carbon power (e.g., $P(\text{C})=22 \text{ W}$, $P(\text{Y})=7.5 \text{ W}$, and $P(\text{NiB})=45 \text{ W}$), YC_2 was also detected in the x-ray diffraction patterns. Most films, which showed a T_c^μ larger than 11 K, also have small amounts of YC_2 impurities.

After optimizing the growth conditions to obtain phase spread alloys containing the 1221 phase with a T_c^μ of 15.1 K, we attempted to change the number of YC planes per Ni_2B_2 plane. To accomplish this the power output of the NiB gun was varied systematically.

Figure 1 shows T_c^μ as a function of the Y/Ni ratio. A given Y/Ni ratio may have several different critical temperatures T_c^μ , due to variations in the B and C contents. The highest T_c^μ (up to 15.1 K) is observed in samples with an Y/Ni ratio of approximately 1/2. For Y/Ni ratios deviating from 1/2, there is a clear decrease of the critical temperatures.

Figure 2 shows x-ray diffraction data for various Y-Ni-B-C phase spread alloys with different Y/Ni ratios. Clearly the 1221 phase is present in the films with an Y/Ni ratio of 0.15 and 0.54, while the 1111 phase is dominant in the film with an Y/Ni ratio of 1. For the film with a Y/Ni ratio of 2 it was not possible to identify the dominant phase from the x-ray diffraction. Remarkably, the films with an Y/Ni ratio around 0.15 show no traces of the 1441 phase in the x-ray diffraction pattern,⁷ but instead show the presence of the 1221 phase. In general, Y-Ni-B-C phase spread alloys with a T_c^μ above 7 K show traces of the 1221 phase, even if their

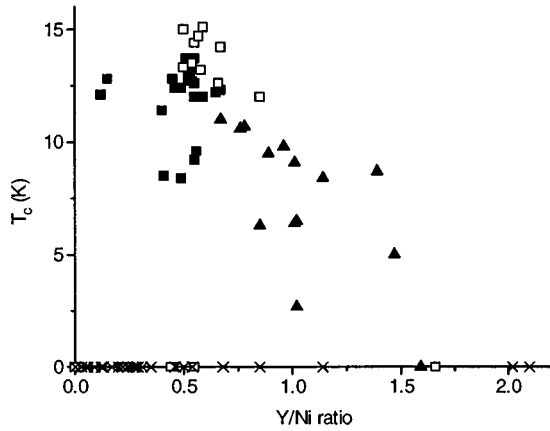


FIG. 1. T_c^μ (from MFM) vs Y/Ni ratio (determined by EDX) for films grown at 900 °C. The dominant phase, determined by x-ray diffraction, is marked with different symbols (1221: squares, 1111: triangles, unidentified: crosses). Solid symbols indicate as grown samples, while open symbols refer to postannealed samples.

Y/Ni ratio deviates significantly from 1/2. The samples with an Y/Ni ratio ranging from 0.7 to 1.5 showed predominantly the presence of the 1111 phase and a strongly reduced T_c^μ . The clear evidence of the 1111 phase in the x-ray data shows, that although deposition parameters (e.g., the substrate temperature) were optimized for the 1221 phase growth, it is possible to grow other phases in the Y-Ni-B-C system by varying the relative power settings of the different sputtering guns. Of course, it may still be the case that under considerably different substrate temperature a yet undiscovered phase may be present.

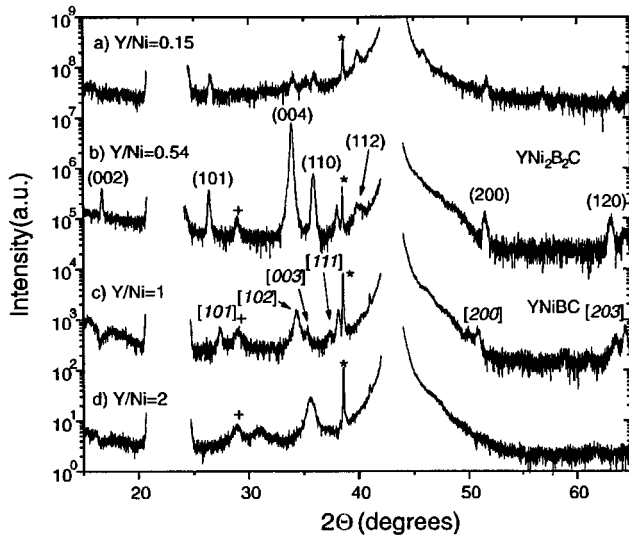


FIG. 2. X-ray diffraction patterns of four samples with different Y/Ni ratios. The different diffraction patterns are shifted relative to each other by factors of 100. T_c^μ are: (a) 12.8 K, (b) 13.5 K, (c) 6.4 K, and (d) 0 K. For clarity the main MgO (100) and (200) substrate peaks were eliminated, and the K_β MgO (200) reflections are indicated with an asterisk (*). The $\text{YNi}_2\text{B}_2\text{C}$ (abc) and YNiBC [abc] peaks are marked with the corresponding Miller indices, while a plus sign (+) corresponds to the (002) peak of YC_2 .

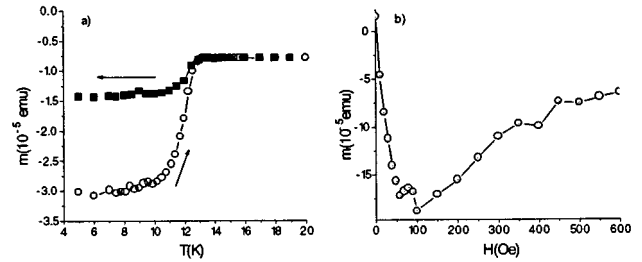


FIG. 3. Magnetization of sample A (Y/Ni=0.57, $T_c^\mu=15.1$ K). (a) Magnetization vs temperature; circles: zero field cooled, squares: field cooled in 5 Oe. (b) Magnetization vs field at 5 K.

Although films predominantly containing the 1111 phase exhibit superconductivity, this does not imply that the 1111 phase is superconducting. Since the MFM microwave absorption is very sensitive, it is possible to detect a signal from superconducting phases which do not show up in the x-ray diffraction. The change of T_c^μ with the Y/Ni ratio suggests that the superconductivity observed in these samples is either due to $\text{YNi}_2\text{B}_2\text{C}$, especially for $T_c^\mu > 10$ K, or to other known binary or ternary compounds, e.g., YC_2 : $T_c=3.8$ K, YB_6 : $T_c=6.5$ K, and YB_2C_2 : $T_c=3.6$ K.¹³

After exploring the different phases of the Y-Ni-B-C system, we attempted the growth of $\text{Y}_x\text{NiB}(\text{C}_{1-x}\text{N}_x)$ by adding nitrogen to the sputtering gas. The incorporation of nitrogen was verified qualitatively from Auger electron spectroscopy, although no crystalline phases were observed in the x-ray diffraction data. None of these films showed any traces of superconductivity. However, due to the lack of clear diffraction evidence, it is not possible to exclude the existence of superconductivity in the crystalline phases of boronitrides.

The magnetization and magnetotransport of the Y-Ni-B-C films with the highest T_c^μ were measured. Figure 3 shows the magnetization as a function of temperature and field for the sample with the highest T_c^μ of 15.1 K and a Y/Ni ratio of 0.57 (sample A). The magnetization versus temperature measurements (see Fig. 3a) were performed in an applied external field of 5 Oe, first zero-field cooled and then field cooled. Above T_c a diamagnetic signal is observed from the MgO substrate. The onset of the film diamagnetic signal gives a critical temperature $T_c^M=12.8$ K, compared to $T_c^\mu=15.1$ K, measured with the more sensitive MFM microwave absorption. We attribute the difference between T_c^M and T_c^μ as resulting from the existence of superconducting phases above 12.8 K which are not detected in the magnetization measurements. In some samples, the magnetization versus applied external magnetic field exhibits several dips (e.g., for sample A at 60 and 100 Oe, see Fig. 3b), possibly due to the presence of other phases or perhaps more interestingly due to dimensional transition in the flux line lattice.^{14,15}

The electrical resistivity of samples A (annealed, $T_c^\mu=15.1$ K, Y/Ni=0.57) and B (as grown, $T_c^\mu=12.8$ K, Y/Ni=0.12) showed superconducting transitions at $T_c^p=14.1$ K and $T_c^p=11.3$ K, respectively, with T_c^p defined as the midpoint of the transition. Again, T_c^p measured by the transport measurements is slightly lower than T_c^μ , due to the need for a percolating network in the resistivity measure-

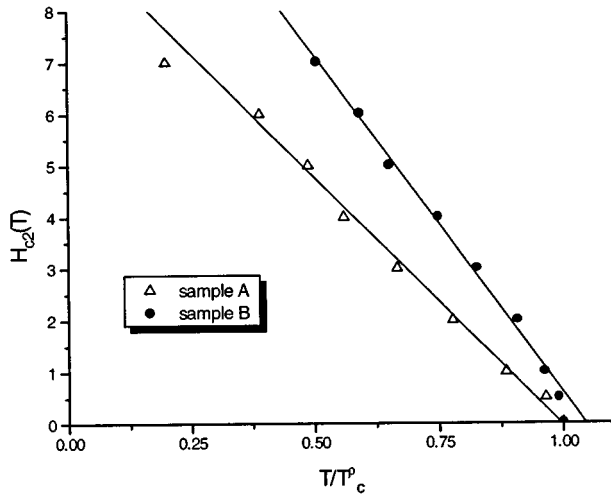


FIG. 4. H_{c_2} vs T for sample A (annealed, $T_c^p=15.1$ K, $Y/Ni=0.57$) and for sample B (as grown, $T_c^p=12.8$ K, $Y/Ni=0.12$). For each sample the temperature is normalized to its zero-field T_c^p . The two solid lines are linear fits to the data below 7 T.

ments. The superconducting transition width is considerably larger in the more inhomogeneous sample B ($\Delta T_c^p=6$ K), than in A ($\Delta T_c^p=1.2$ K). Upon application of an external magnetic field, T_c^p decreased, but ΔT_c^p remained constant for both samples.

The temperature dependence of H_{c_2} , obtained from the magnetoresistance data, is shown in Fig. 4. As expected from the Ginzburg-Landau theory,¹⁶ both samples show a linear temperature dependence of H_{c_2} over a wide temperature range. An upper limit for H_{c_2} at $T=0$ K was obtained from the slope in the linear region¹⁷ below 7 T using:

$$H_{c_2}(T=0) \leq -0.693T_c^p \left(\frac{\partial H_{c_2}}{\partial T} \right)_{T=T_c^p}. \quad (1)$$

In this fashion $H_{c_2}(0)=6.7 \pm 0.3$ T for sample A, and $H_{c_2}(0)=9.1 \pm 0.3$ T for sample B, respectively, with the error estimated from the width of the transition. These data are in good agreement with earlier measurements done on YNi_2B_2C single crystals.^{18,19}

Ovchinnikov and Kresin proposed that layered superconductors with magnetic impurities should have a positive curvature of H_{c_2} , and thus a much higher $H_{c_2}(T=0)$ than expected from Eq. 1.²⁰ Such behavior has indeed been observed for some overdoped high T_c cuprate superconductors with magnetic impurities.²¹ Although YNi_2B_2C has a layered structure and contains magnetic nickel, no such unconventional $H_{c_2}(T)$ behavior is observed in our data (see Fig. 4).

One can also estimate the Landau coherence length λ and penetration depths ξ from the Ginzburg-Landau theory using¹⁶

$$4\pi\lambda^2 H_{c_1} = \phi_0 (\ln(\kappa) + 1/2), \quad (2)$$

$$2\pi\xi^2 H_{c_2} = \phi_0 \quad (3)$$

and

$$2\kappa^2 H_{c_1} - (\ln\kappa + 1/2)H_{c_2} = 0, \quad (4)$$

where $\kappa = \lambda/\xi$ and ϕ_0 is the flux quantum. Solving Eq. 4 numerically for κ , using $H_{c_1}=100$ Oe and $H_{c_2}=6$ kOe for sample A, gives a value of $\kappa=37$, and using Eq. 3, $\lambda=260$ nm and $\xi=7$ nm. These results vary somewhat from sample to sample, with values of $\kappa=15-40$, $\lambda=120-300$ nm, and $\xi=5-10$ nm. This data is in good agreement with other measurements on bulk YNi_2B_2C single crystals, where values of $\lambda_{ab}=150$ nm and $\xi_{ab}=10$ nm were reported.¹⁸

IV. CONCLUSION

We have applied a phase spread alloy technique (DSPM) to search for new superconductors in the Y-Ni-B-C system. Films with different Y/Ni ratios ranging from 0.1 to 2.3 were obtained, and superconductivity above 7 K, with a maximum T_c of 15.1 K, could be attributed to a polycrystalline YNi_2B_2C (1221) phase. Films with a Y/Ni ratio of approximately 1 were predominantly composed of polycrystalline $YNiBC$, although the superconductivity may be due to binary or ternary impurities or traces of the YNi_2B_2C phase. Films with a Y/Ni ratio higher than 1.6 were not superconducting. Therefore, besides YNi_2B_2C , no new phase with a T_c above 10 K was found in the Y-Ni-B-C system. Moreover, no superconductivity was detected in films grown with nitrogen added to the sputtering gas, to grow $Y_xNiB(C_{1-z}N_z)_y$ compounds. Finally, magnetization and magnetoresistance data of the films with the highest T_c 's show conventional type II superconducting behavior.

ACKNOWLEDGMENTS

The authors thank Professor K. Andres for arranging the participation of B. Knigge in this work and R. J. Cava, T. Endo, D. Mendoza, J. Santamaria, and M. Velez for useful discussions and comments. Furthermore, the authors thank R. J. Cava for providing them with a bulk YNi_2B_2C sample to calibrate their EDX measurements. This work was supported by the Electric Power Research Institute, and NSF-DMR-96-23949.

¹ See, for instance, K. Kitazawa, *Physica C* **235-240**, R23 (1994).

² D. Lederman, D. C. Vier, D. Mendoza, J. Santamaria, and I. K. Schuller, *Appl. Phys. Lett.* **66**, 3677 (1995).

³ R. J. Cava, H. Takagi, B. Batlogg, H. W. Zandbergen, J. J. Krajewski, W. F. Peck, Jr., R. B. van Dover, R. J. Felder, T. Siegrist, K. Mizuhashi, J. O. Lee, H. Eisaki, S. A. Carter, and S. Uchida, *Nature (London)* **367**, 146 (1994).

⁴ R. Nagarajan, C. Mazumdar, Z. Hossain, S. K. Dhar, K. V. Gopalakrishnan, L. C. Gupta, C. Godart, B. D. Padalia, and R. Vijayaraghavan, *Phys. Rev. Lett.* **72**, 274 (1994).

⁵ R. J. Cava, H. Tagaki, H. W. Zandbergen, J. J. Krajewski, W. F. Peck, Jr., T. Siegrist, B. Batlogg, R. B. van Dover, R. J. Felder, K. Mizuhashi, J. O. Lee, H. Eisaki, and S. Uchida, *Nature (London)* **367**, 252 (1994).

⁶ A. K. Gangopadhyay and J. S. Schilling (to be published).

⁷ Q. W. Yan, B. G. Shen, Y. N. Wei, T. Y. Zhao, Y. S. Yao, B. Yin, C. Dong, F. W. Yang, Z. H. Cheng, P. L. Zhang, H. Y. Gong, and Y. F. Li, *Phys. Rev. B* **51**, 8395 (1995).

⁸ T. Siegrist, H. W. Zandbergen, R. J. Cava, J. J. Krajewski, and W. F. Peck, Jr., *Nature (London)* **367**, 254 (1994).

- ⁹C. N. R. Rao, in *High Temperature Superconductivity and Other Related Topics*, edited by B. E. Baaqie, C. K. Chew, C. H. Cai, and C. H. Oh (World Scientific, Singapore, 1989), p. 195.
- ¹⁰R. J. Cava, H. W. Zandbergen, B. Batlogg, H. Eisaki, H. Tagaki, J. J. Krajewski, W. F. Peck, Jr., E. M. Gyorgy, and S. Uchida, *Nature (London)* **372**, 245 (1994).
- ¹¹I. N. Chan, D. C. Vier, O. Nakamura, J. Hasen, J. Guimpel, S. Schultz, and I. K. Schuller, *Phys. Lett. A* **175**, 241 (1993).
- ¹²S. Arisawa, T. Hatano, K. Hirata, T. Mochiku, H. Kitaguchi, H. Fujii, H. Kumakura, K. Kadowaki, K. Nakamura, and K. Togano, *Appl. Phys. Lett.* **65**, 1299 (1994).
- ¹³*Landolt Börnstein Numerical Data and Functional Relationships in Science and Technology Group III*, New Series, Vol. 21, edited by O. Madelung (Springer, Berlin, 1993).
- ¹⁴For dimensional transition in the flux lattice of conventional superconductors see: J. Guimpel, L. Civale, F. de la Cruz, J. M. Murduck, and I. K. Schuller, *Phys. Rev. B* **38**, 2342 (1988).
- ¹⁵For dimensional transition in the flux lattice of high T_c superconductors see: C. Hünnekes, H. G. Bohn, W. Schilling, and H. Schulz, *Phys. Rev. Lett.* **72**, 2271 (1994).
- ¹⁶See, e.g., M. Tinkham, *Introduction to Superconductivity*, 2nd ed. (McGraw-Hill, New York, 1996).
- ¹⁷N. R. Werthamer, E. Helfand, and P. C. Hohenberg, *Phys. Rev.* **147**, 295 (1966).
- ¹⁸M. Xu, P. C. Canfield, J. E. Ostensen, and D. K. Finnemore, *Physica C* **227**, 321 (1994).
- ¹⁹M. Xu, B. K. Cho, P. C. Canfield, D. K. Finnemore, and D. C. Johnston, *Physica C* **235–240**, 2533 (1994).
- ²⁰Yu. N. Ovchinnikov and V. Z. Kresin, *Phys. Rev. B* **52**, 3075 (1995).
- ²¹A. S. Alexandrov, V. N. Zavaritsky, W. Y. Liang, and P. L. Nevsky, *Phys. Rev. Lett.* **76**, 983 (1996).